

Quantification and classification of retinal vessel tortuosity

Rashmi Turior*, Danu Onkaew, Bunyarit Uyyanonvara, Pornthep Chutinantvarodom

Sirindhorn International Institute of Technology, Thammasat University, 131 Moo 5, Tiwanont Road, Bangkadi, Muang, Pathumthani 12000 Thailand

*Corresponding author, e-mail: rashmi.turior@siit.tu.ac.th

Received 18 Jul 2012

Accepted 25 Mar 2013

ABSTRACT: The clinical recognition of abnormal retinal tortuosity enables the diagnosis of many diseases. Tortuosity is often interpreted as points of high curvature of the blood vessel along certain segments. Quantitative measures proposed so far depend on or are functions of the curvature of the vessel axis. In this paper, we propose a parallel algorithm to quantify retinal vessel tortuosity using a robust metric based on the curvature calculated from an improved chain code algorithm. We suggest that the tortuosity evaluation depends not only on the accuracy of curvature determination, but primarily on the precise determination of the region of support. The region of support, and hence the corresponding scale, was optimally selected from a quantitative experiment where it was varied from a vessel contour of two to ten pixels, before computing the curvature for each proposed metric. Scale factor optimization was based on the classification accuracy of the classifiers used, which was calculated by comparing the estimated results with ground truths from expert ophthalmologists for the integrated proposed index. We demonstrate the authenticity of the proposed metric as an indicator of changes in morphology using both simulated curves and actual vessels. The performance of each classifier is evaluated based on sensitivity, specificity, accuracy, positive predictive value, negative predictive value, and positive likelihood ratio. Our method is effective at evaluating the range of clinically relevant patterns of abnormality such as those in retinopathy of prematurity. While all the proposed metrics are sensitive to curved or kinked vessels, the integrated proposed index achieves the best sensitivity and classification rate of 97.8% and 93.6%, respectively, on 45 infant retinal images.

KEYWORDS: k -curvature, improved chain code, retinopathy of prematurity

INTRODUCTION

Retinal fundus images provide important information for early detection of many retinal and systemic diseases. Examination of the appearance of the retinal blood vessels is therefore of immense clinical importance. Buckling in the blood vessel network of the retina may be due to dilation (radial stretching in the vessels) or longitudinal stretching. They are markers of not only retinal pathologies but also of other systemic diseases originating in the cardiovascular, central nervous, and endocrine-metabolic systems¹. Twisted appearance of vessel course is rightly termed as tortuosity. Increase in vessel tortuosity is the first manifestation of the changes in vessel morphology. Tortuosity could be produced due to several causes akin to high blood flow, angiogenesis, or blood vessel congestion. It could be concentrated or focal or stretch along the entire retinal vasculature.

Since tortuosity feature is a very important cue for eye diseases, its severity and progression with time, there is a need for the measurement of tortuosity in

a consistent, repeatable manner. A basic ability to investigate the sign of disease would be to detect the vascular structure and measure the tortuosity. Hence this paper concentrates on the task of vessel detection and tortuosity measurement of vascular structure in retinal fundus images.

Tortuosity has been shown to be a more reliable vascular parameter in differentiating retinopathy of prematurity (ROP) severity than vessel width². ROP is a developmental disease of eye in premature infants characterized by increased dilation and tortuosity of the retinal blood vessels. The exact causes of ROP are not completely understood, however it could be classified into three stages as active, non active, and very active ROP. The tortuosity attribute provides relevant estimates of the degree of prematurity.

Several possible measures of tortuosity and vessel diameter have been proposed^{3–5} (each with its own constraints). However, relatively few attempts^{6–8} have been made to quantify tortuosity in case of infant retinal blood vessels. In order to assess the clinical significance of tortuosity changes with time and to

relate different levels of the same retinopathy, there is a dire need to devise a new approach for tortuosity evaluation that matches the clinical perception of ophthalmologists.

Tortuosity evaluation relevant to the clinical acuity of the ophthalmologists still remains an open problem and varies from disease to disease³. Grading of tortuosity in clinical practice is usually done using a gross qualitative scale (e.g., mild, moderate, severe and extreme)⁶; as a result the analysis remains subjective. A reliable quantitative measure would provide an objective assessment thereby enable the automated measurement of retinal vascular tortuosity and its progression to be more easily discerned. A range of tortuosity measure based on ratio of the arc length and chord length^{4,7}, was commonly used^{5,8,9}, though it was recognized as inconsistent²; since it provided similar numeric values for a gradual bending vessel and for the one that bends more frequently. Automated measurement using seven integral estimates of tortuosity based on the curvature of vessels was formulated⁵. However, it could not differentiate the tortuosity of structures that had different perceived tortuosity. This was generalized to 3D images obtained by means of the magnetic resonance angiography to achieve better accuracy of tortuosity calculation³. Measurement of tortuosity based on relative length variation was proposed¹⁰, which include relationships between tortuosity, diameter and pressure which produce change in the shape of artificial latex vessels. Measurement of tortuosity by using Fourier analysis was proposed long ago¹¹ but Fast Fourier transform of the vessel's curvature as a measure of tortuosity has been introduced lately¹². Method to compute tortuosity using second derivatives along central axis of the blood vessels was proposed¹³. An interface based on MIDAS was developed¹⁴, but it proved to be subjective and time consuming. Few authors¹⁵ proposed to measure vessel diameter using two different methods to estimate profile width, but in this case bifurcations and crossings were not considered while choosing the vessel segment. Then an alternative method to calculate tortuosity of each individual segment was proposed¹⁶. The idea behind is to use the points of changing curvature sign. Nonetheless, this algorithm required manual vessel tracing and it cannot distinguish tortuosity of vessel with constant curvature. In Ref. 17, the length of the smooth curve was estimated by choosing points along the vessel that were about 40 pixels apart, and tortuosity was evaluated by the ratio of the total length of the vessel to the length of the smooth curve. It was assumed that it gives a more accurate measure of tortuosity. However,

in this study the plus disease threshold value had to be set a priori at a tortuosity index of 9 because it proved more accurate in pilot studies. Lately, computer-aided image analysis of the retina was developed for the measurement of tortuosity and width of retinal veins and arteries using simulated vessels¹⁸. Robust metrics employing unit speed parametrization for quantifying vascular tortuosity in terms of 3-D curvature is also defined¹⁹.

In previous work, we have defined and evaluated methods for automatic measurement of retinal vessel tortuosity in infant retinal images using PCA²⁰ and combination of inflection count and curvature of improved chain code²¹, and curvature based on chain code rules²². In experiments on comparable data sets, the accuracy for these methods was 100%^{21,22}. While these results are encouraging, they are limited by suboptimal feature selection and unsupervised classification techniques. Here, we take a machine learning approach to the problem of tortuosity classification. Our method performs tortuous vessel feature selection and classification using a naïve Bayes (NB) classifier and a nearest neighbour (NN) classifier. We preprocess the images to extract the blood vessel network, remove noise, reduce it to a single pixel skeleton network, segment it into sub vessel samples, calculate tortuosity by the proposed approach, then classify those features using a model built from a training set.

Any proposed measure must satisfy some intuitive properties to procure clinical recognition of a valid tortuosity metric. To make it explicit, any measure should be invariant to similarity transformations of a vessel: translation, rotation, and scaling. The position and orientation of a vessel do not affect the perception of tortuosity; nor should the scaling, so that the image of a vessel can be viewed at different resolution without affecting its perceived degree of tortuosity. However, if scale does affect, (that is scale space transformation), it does so in multiples. A valid tortuosity measure should be sensitive to changes in the patterns of the vessel, i.e., to the shape of its path in space. It should be susceptible to the amplitude and changes in convexity (twists) of the vessel, collectively termed as modulation property. An ideal index should be additive, i.e., the tortuosity of a composite vessel, consisting of several parts, should be equal to the sum of the tortuosity of those parts.

This paper proposes a suite of tortuosity metrics based on curvature calculated by improved chain-code. The curvature estimate is based on proper pairing of chain codes and related chain-code rules. We give a brief overview of the method and refer the readers to Ref. 23 for further details. Earlier

proposed measures on curvature^{5,24} were not well-defined because they used arbitrary parametrization. To avoid this, work based on certain geometric concepts related with straightness and non-straightness of a digital curve is employed. This is realized efficiently with chain code representation. The measure of k -curvature, used in Ref. 25 for the detection of high curvature points referred to as corners or dominant points, has been modified in three stages in Ref. 23. It is used in the proposed approach to achieve an appreciable improvement for evaluating the curvature of arbitrary shaped vessel curve. The basic problem dealing with 2D projection images is that vessel crossings cannot be resolved. This problem is taken care of by proposing a new method for vessel partitioning based on improved branching and ending point detection technique. It is to be noted that for 2D data sets an estimation of dilation as well as tortuosity is required to completely define the morphology of the vessel network.

The efficacy of the proposed metrics in matching the medical insight of tortuosity is investigated using simulated curves of varying curvatures and shapes and infant retinal images at different resolutions. We demonstrate that our proposed metrics preserve additive property, modulation, and sensitivity to shapes. One of the proposed measures is invariant to scale.

MATERIALS AND METHODS

Putative tortuosity indices

The most prevalent index of tortuosity, probably because of its conceptual simplicity and ease of computation, is the arc-chord ratio factor^{4,7} (referred as L-C in this study). It has a value of unity for a straight vessel and increases with vessel elongation. However, it provides no information as regards the morphology or haemodynamic consequences and fails to differentiate between vessels of similar arc length but different perceived tortuosity. It only indicates vessel elongation, since it depends on total curve length independent of shape.

Other putative indices include measures that involve the use of the integral of the absolute curvature (tc) or of the squared curvature (tsc)⁵. These involve direct measurement of discrete curvature or functions of discrete curvature. The idea behind this is to measure the variability in vessel direction. Another approach based on second differences of the coordinates of the vessel midline (TC) was proposed¹³. All these metrics required a somewhat arbitrary smoothing scheme or a sufficiently high sampling frequency during digitization and do not consider the changes in

the convexity of the curve, i.e., the curvature sign is not taken into account.

A tortuosity metric based on the number of inflection points (twists) was proposed^{3,24} to incorporate changes between smoothly curved vessel and vessels that make abrupt changes in direction. It was referred as the Inflection Count Metric (ICM), defined in terms of the ratio of the straight-line distance between the end points of the vessel C to the meandering vessel length L . Specifically

$$\text{ICM} = (n_{\text{ic}} + 1)C/L,$$

where n_{ic} is the number of twists.

However, it failed in depicting the clinician's perception of tortuosity, since evaluation of retinal tortuosity by humans is based more on the local winding of a vessel than on an overall difference between a straight line and the curve under examination.

Proposed tortuosity metrics

Definitions: A vessel is defined as a curve

$$y = f(x) : D \subset R \rightarrow R$$

with $y \in R$ and the coordinates of y defined on an interval domain D of R . The chord length C is defined as the distance between the end points of the curve and the arc length L is the distance along the curve. The curvature at a point $p(x, y) \in R$ is expressed as

$$\kappa(p) = \frac{y''}{(1 + y'^2)^{3/2}}, \quad (1)$$

where y' and y'' are the first and second derivative with respect to x , respectively.

For a digital curve, small changes in slope are difficult to estimate by (1), simply by replacing the derivatives by first-and-second order differences ($k = 1$), since the successive vectors for such a curve differ in direction only by a multiple of 45° . This problem is overcome by considering the differences for $k > 1$, i.e., a smoothed version of discrete curvature is measured as in Refs. 23, 25. This k -curvature measure is defined as the difference in mean angular direction of k vectors (eq. (3.2) of Ref. 25) on the leading and trailing curve segment of the point of interest, p_i , is marked by its provision of modifying the value of k . The decision is based on k pair of chain codes, k is relatively a small integer in the interval $[1, 16]$. Smaller value of k considers smaller number (e.g., $k = 6$) of points leading to and following p_i , thus overlooking the parts of the curve lying far off from p_i (Fig. 1). On the other hand, a large value of k , allows

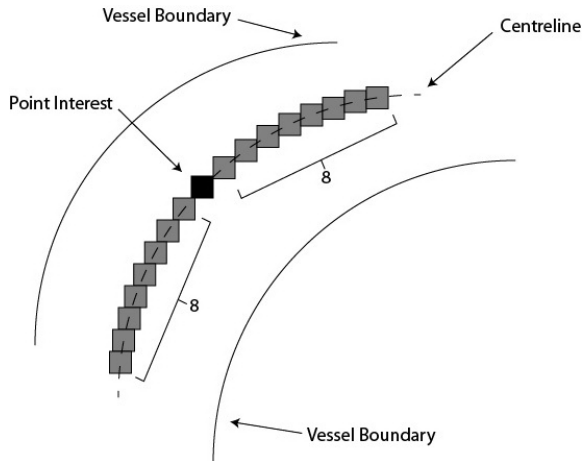


Fig. 1 A segment of a digital curve showing pair of chain codes for $k = 8$.

a large number of points to decide the curvature at p_i . The discrete curvatures are estimated using the flow pattern of the constituent curve points in and around the concerned point, p_i , by:

$$\kappa(p_i, k) = \frac{1}{k} \sum_{j=1}^k \min \left\{ \begin{array}{l} \min(f'_{i+j}, 8 - f'_{i+j}), \\ \min(f'^{(+1)}_{i+j}, 8 - f'^{(+1)}_{i+j}), \\ \min(f'^{(-1)}_{i+j}, 8 - f'^{(-1)}_{i+j}) \end{array} \right\}, \quad (2)$$

where

$$\begin{aligned} f'_{i+j} &= |f_{i+j} - f_{i-j+1}|, \\ f'^{(+1)}_{i+j} &= |f_{i+j+1} - f_{i-j+1}|, \\ f'^{(-1)}_{i+j} &= |f_{i+j} - f_{i-j}|. \end{aligned}$$

f_{i+j} and f_{i-j} are the chain code of the j th leading and following point with respect to point of interest p_i , respectively (refer to eq. (5) in Ref. 23), where f_{i+j} is an integer given by $f = 0, 1, 2, \dots, 7$. k is the number of points used for curvature calculation, it can be viewed as a smoothing parameter. In this work, the value of k is experimentally determined. The value of k can be varied for more accuracy of curvature depending upon the applicability, but it leads to increase in computational cost.

Curvature-based metrics

Curvature estimation is a vital task in shape analysis in general, and tortuosity evaluation in particular. The most important parameter characterizing tortuosity is the curvature of the blood vessel. However, integration of the curvature along the blood vessel is not the best option, since on average the curvature might

not be very large, but it can be large along certain part of the vessel. Hence in this paper, replicating ophthalmologists' notion, we comprehend tortuosity as points of high curvature of the blood vessel along a certain segments.

In Ref. 16 the curve is partitioned into segments using the points where the curvature changes the sign, referred as turn points. On the contrary, our method is based on evaluating the tortuosity by estimating curvature of each point over some region of support (2), i.e., is determined by using the neighbouring points within the extent, and then summing curvature at every pixels of the vessel. We believe that this procedure closely resemble the manner the humans evaluate tortuosity. We previously defined tortuosity metrics, K_{tc} and K_{tsc} ²², in terms of curvature and squared curvature given by

$$\begin{aligned} K_c &= K_{sub} = \sum_{i=1}^n \kappa(p_i, k), \\ K_{sc} &= \sum_{i=1}^n \kappa^2(p_i, k), \end{aligned}$$

where n is the number of pixels in each segmental vessel samples. The curvature at each point is calculated by (2) and is squared and then summed together to get the squared curvature of a curve. The total curvature and the total squared curvature of the blood vessel network is given by

$$K_{tc} = \sum_{j=1}^N K_c, \quad (3)$$

$$K_{tsc} = \sum_{j=1}^N K_{sc}, \quad (4)$$

where N = number of segmental vessel (a segment of the vessel tree delimited by two end points or a branch point and an end point) samples in the whole vascular network. K_c and K_{sc} represent curvature and squared curvature of each vessel curve. For large N , the sum is equivalent to numerical integration.

Note that for $k = 1$, K_c becomes the measure recommended by Hart et al⁵.

Integrated proposed index

We proposed an efficient technique based on curvature calculated from improved chain-code to estimate the tortuosity of blood vessel²¹ expressed as

$$\tau = \left(\frac{n_{ic} - 1}{n_{ic}} \right) \frac{1}{L} \sum_{i=1}^n \kappa(p_i, k), \quad (5)$$

where n_{ic} and L are the number of inflection points and arc length, respectively; n is the number of pixels in the segmental vessel considered. The proposed index takes a value of zero when n_{ic} is equal to 1 (a smoothly curved vessel with no change in curvature sign), and is always greater than zero when the curvature changes sign.

In this integrated proposed index, the number of inflection or twists points is taken into account to distinguish between smoothly curved blood vessel and vessels that make abrupt changes in direction. Inflection points of a vessel curve is defined as the curvature value decreases to zero, similar to a change in sign of the curvature for planar curves (curvature of a curve defined as in (2)). To overcome small oscillations (that perhaps affect the precise inflection number of the vessel) along the vessel that occur due to noise, we set threshold on curvature (in this study threshold = 0.18).

This index has an advantage over arc-chord ratio which fails to distinguish between long segments as it does not analyse tortuosity along the segments.

The index produces the expected estimate irrespective of the fact that the concerned point has an extreme curvature or the concerned segment has a constant or changing curvature unlike the metric proposed by Grisan et al¹⁶. To allow comparison of vessel of different length, a normalization factor is introduced. This method alleviates the problem associated with the method used for vessel segmentation, that is, it is independent of the vessel sub segmentation. Moreover, it takes into account both, the number of inflection points (twists) and amplitude of each segmental-vessel.

Experiments

Performance of the proposed tortuosity indices are tested and compared with other available indices, (L-C and ICM in this study), by experiments that are performed in two phases.

In the first phase, vessels are simulated in different forms to evaluate the compliance of various methods with the abstract properties of tortuosity. Values for the proposed indices (τ , K_{tc} , and K_{tsc}) are calculated for each case. K_{tc} and K_{tsc} are the tortuosity based on total curvature and total squared curvature as expressed by (3) and (4), respectively. τ is the tortuosity measure as defined by (5).

In the second phase, we further extend our experiments using a suite of proposed metrics. We use K_{tc}/L , K_{tc}/C , K_{tsc}/L , and K_{tsc}/C as length-normalized measures. In this part, vessel centreline of a set of retinal images from infant retina is extracted

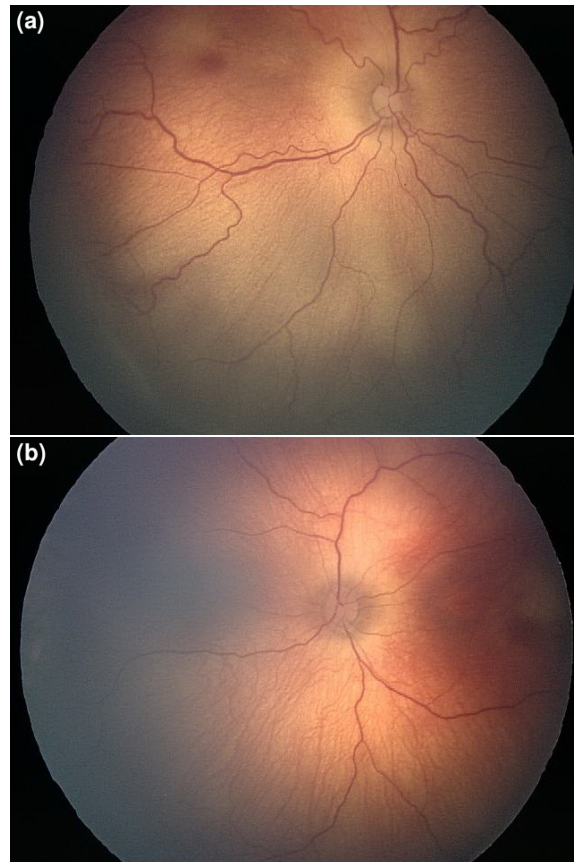


Fig. 2 The example images from (a) tortuous image, (b) normal image.

and segmented according to improved branching point and ending point detection technique and analysed by the proposed indices. The results are verified by two expert ophthalmologists.

Simulated vessels

To test the variations in the performance of the various proposed tortuosity measures when single parameters that influence the clinical acumen of tortuosity changes, various sine waves and derived shapes are simulated with same frequency f (or time period T) and chord length L , but different amplitude A , $A \in \{15, 25, 30, 40, 50\}$, $L \in [0, 128]$, $f = 1$ or $T = 1$; and with the same amplitude A and chord length L , but different frequency f ; $A = 15$, $L \in [0, 128]$, $f \in \{\frac{1}{2}, 1, \frac{3}{2}, 2\}$ or $T \in \{2, 1, \frac{2}{3}, \frac{1}{2}\}$.

Processing of retinal images

Image acquisition: In this work, images were obtained from Digital Imaging Research Centre, Kingston University, London, Department of Ophthal-

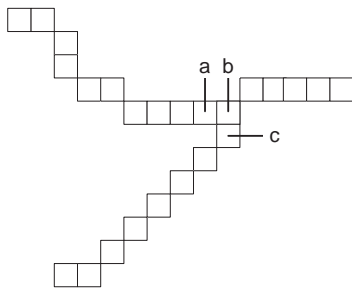


Fig. 3 A digital curve vessel segment.

mology, Imperial College, London and Thammasat Hospital, Thailand. The example of retinal images in ROP infants are (Fig. 2). They are representative samples of a set of normal retinal images and abnormal ones taken from infant born at mean gestational age of 28.5 ± 1.0 week and with a mean birth weight of 1080 ± 80 g. The images were captured by Ret Cam 120 digital camera. The system produced images of 640×480 pixels of 24 bit RGB bitmaps. All images were JPEG compressed.

Description of images: Images of 60 eyes from 50 different infants (right eye of 40 different infants and both eyes of 10 different infants) screened during 18–24 months time period were graded by two expert ophthalmologists. The experts graded the images as normal, mild and extreme tortuous following the international classification of ROP revisited²⁶.

Image preprocessing

Before tortuosity calculation, image preparation is required. Infant images usually have low contrast; therefore, to extract centreline of blood vessel, the Laplacian of Gaussian to grey scale of an RGB image is applied, followed by Otsu thresholding. Then, a set of morphological operations were carried out following to the technique by Lassada et al⁹ to eliminate noise and get a single-pixel skeleton of the vessel tree.

Next, vessel partitioning is done by using improved branching and ending point detection technique. Consider a segment of a digital curve (Fig. 3). We track every vessel pixel and count the number n of pixel around the eight neighbour of a current location that has the same intensity as vessel pixel, and use this number to classify the point as ending point ($n = 1$), non-significant point ($n = 2$), and candidate for branching point ($n \geq 3$). Branching point is defined as n more than or equal to 3²⁷. Yet, the results are flawed sometimes. In this study, we, compute four connectivity of each eight neighbour of

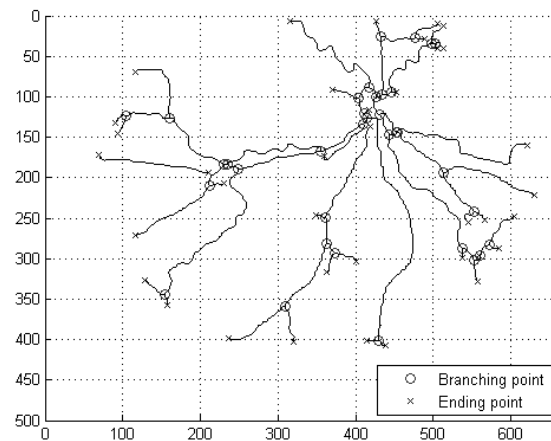


Fig. 4 Branching and ending point detection.

branching point candidate (ignore the branching point candidate). If there is no connectivity in each eight neighbour, that branching point candidate is masked as a branching point. In this case only point b is considered as a branching point. Results of branching point and ending point detection are shown in Fig. 4.

Tortuosity calculation

The quantitative definition of tortuosity in medical literature still remains vague. We propose an integrated measure, τ and a suite of tortuosity metrics based on curvature calculated from improved chain code rules. To calculate curvature at each point on curve, we applied the improved algorithm for estimating k-curvature described in Pal et al²³. A window size of 17 pixels achieved optimal results in our experiments with ROP images. The window size was determined experimentally by observing the curvature, K_{tc} , K_{tsc} , as well as the τ values obtained with vessel contours over a window of size 5, 7, 9, 11, 13, 15, 17, 21. Nevertheless, this figure will vary for different image resolutions. Tortuosity of all the vascular branches was used in the calculations to avoid discrepancies in the identification of arterioles and venules with respect to clinical perception.

Classification

In our experiment, the classification is segmental (segment-based), so each training or test sample represents one segment of the vessel in training and testing set. Segmental vessels are assigned to one of the three tortuosity classes, viz-a-viz; non, semi and extreme tortuous class. Two experts were asked to grade each of the segmental vessels into three classes of tortuosity. Their judgement is based wholly on their

experience and knowledge. A data set of 60 images, made up of 2176 segmental vessels, depicting a range of image quality and image type was given to the two expert ophthalmologists for grading. The dataset consists of images varying from fundus photos showing no ROP to those exhibiting advanced ROP. The two experts had difference in opinion for 15 infant images (broken down into 676 segmental vessels), that is to say, that there was inter-expert disagreement in the three tortuosity classes, therefore these are excluded from this study and only 45 infant images (comprising 1500 segmental vessels) are used for analysis. Out of these 45 images, 5 images are determined to have plus diseases, indicating advanced ROP, 19 images are suspected of pre-plus disease and the rest 21 images shows no-plus disease, indicating no ROP. These 45 images comprise images of right eye from 35 different infants and both eyes of 5 infants. The 45 images are the Ground truth data that is obtained from the agreed judgement of two expert ophthalmologists. As a simple baseline for comparison, we experiment with two classifiers: the NB classifier and NN classifier.

The NB classifier^{28,29} is the optimal method of supervised learning if the values of the attributes of an example are independent given the class of the example. It estimates prior probabilities by calculating simple frequencies of the occurrence of each feature value given each class, then return a probability of each class, given an unclassified set of features.

Bayes' theorem relates on Bayes' rule of a hypothesis y and a finite set of features x which bears on the hypothesis, then

$$P(y|x) = (P(x|y)P(y))/P(x) \quad (6)$$

where $P(y|x)$ is the parameter we want to estimate and $P(y)$ is the probability of class y . $P(x|y)$ is the likelihood of feature x given class y , $P(x)$ is an independent probability of feature x .

The NB classifier uses the principle of Bayesian maximum a posteriori classification: measure the feature data then select the class:

$$\hat{y} = \arg \max_y P(y|x).$$

Bayes' theorem is used in NB classifier to find $P(\text{tortuous class}|\text{tortuosity value})$ as $(P(\text{tortuosity value}|\text{tortuous class})P(\text{tortuous class}))/P(\text{tortuosity value})$. Here 'tortuous class' can be non-tortuous, semi-tortuous, or extreme-tortuous. We estimate the parameters $P(x|y)$ and $P(y)$ from training data.

The NN classifier classifies a test instance with the class of the nearest training instance according to two

distance measures, Mahalanobis and Euclidean. We use Euclidean distance method ($k = 4$) to measure the distance between the test instance and training data:

$$\text{Distance}(x, y) = \left[\sum_{i=1}^n (x_i - y_i)^2 \right]^{1/2}, \quad (7)$$

where x is the feature data vector of retinal vessel we want to classify, y is the feature data vector of retinal vessel in the training data set, x_i is the feature data of retinal vessel we want to classify, and y_i is the feature data of retinal vessel in the training data set.

Since we have nine metrics showing the tortuosity level, we use all of them as a feature vector of the retinal vessel for classification.

After finding all k instances retinal vessel in the training data set, that has minimum distance to the retinal vessel we want to classify, we determine the class of retinal vessel by simply counting on the k instances. The retinal vessel should belong to the class having the maximum number of the k instances.

The data set of 45 images is split into training and test set. The training set consists of 33 images comprising 1075 segmental vessels consisting of 896 non tortuous samples, 140 semi tortuous samples and 39 extreme tortuous samples. The test set is made up of 12 images broken down into 425 segmental vessels consisting of 350 non tortuous samples, 50 semi tortuous samples and 25 extreme tortuous samples.

Selecting a value for k

We compute the curvature κ at a point p_i lying in a locally straight segment, using (2), such that the error due to inherent jaggedness of a digitally straight piece is minimized. For example, in Fig. 3, we get $\kappa(a, 4) = (0 + 0 + 0 + 0)/4 = 0$ and $\kappa(b, 4) = (0 + 0 + 0 + 0)/4 = 0$, which conforms to the fact that a and b lie on a straight piece (w.r.t. $k = 4$). However, $\kappa(c, 4) = (2 + 0 + 0 + 0)/4 = 0.5$, which is alarmingly low, as point c lies in the region of high curvature. When curvature is computed for $k = 8$ as $\kappa(c, 8) = (3 + 3 + 3 + 3 + 3 + 4 + 4 + 4)/8 = 3.375$. Thus we get improvement over $\kappa(c, 4) = 0.5$. Also for point b , $\kappa(b, 8) = (4 + 4 + 4 + 4 + 3 + 4 + 2 + 2)/8 = 3.375$, which supports the fact that b and c are dominant points or corner points with high curvature values. Besides, we try to show the classification accuracy over increasing values of k using two classifiers for our integrated proposed measure. Table 1 depicts the classification rates, i.e., the proportion of the total number of correctly classified predictions. The authors believe that a vessel of 10 pixels or less is considered too small for tortuosity evaluation, thus

Table 1 Classification accuracy of our integrated proposed tortuosity metric, τ , for different values of k with NB and NN classifiers.

k	2	3	4	5	6	7	8	10
τ , NB	71.4	80.7	74.3	78.6	85.0	85.3	91.4	89.3
τ , NN	68.6	80.7	82.9	81.4	85.7	87.9	93.6	86.4

perhaps provide misleading results. We find that the maximum classification rate achieved, is for $k = 8$ using both the classifiers. We observe that increasing the value of k further decreases the classification rate of at least one class. These observations form the basis on which $k = 8$ is the best value predicated in the present work.

Performance measurement

We evaluate performance on the test set quantitatively by comparing the classifiers' result to ground truth.

To assess classifiers' performance, we use sensitivity, specificity, accuracy, positive predictive value (PPV) and negative predictive value (NPV) on a segmental basis. We also use positive likelihood ratio (PLR) to access the performance of each classifier for each of the tortuosity indices. All measures are calculated based on four values namely the true positive rate (the number of extreme and semi tortuous segmental vessels correctly classified), the false positive rate (the number of non tortuous segmental vessels wrongly classified as semi or extreme tortuous segmental vessels), the false negative rate (the number of semi and extreme tortuous segmental vessels not classified) and true negative rate (the number of non tortuous segmental vessels correctly classified as non tortuous segmental vessels).

Sensitivity is the percentage of actual semi and extreme tortuous segmental vessels that are detected; specificity is the percentage of non tortuous segmental vessels that are correctly classified as non tortuous segmental vessels. Accuracy is the overall success rate of the classifiers. It gives the proportion of the test samples that are correctly classified. The PPV is the number of extreme, semi tortuous segmental vessels and non-tortuous segmental vessels that are positively detected and NPV is the proportion of extreme, semi tortuous segmental vessels and non-tortuous segmental vessels that are negatively detected. They are the (conditional) probabilities of the segmental vessel being semi or extreme tortuous given that the test result is positive (PPV), or non tortuous when the test result is negative (NPV). The PLR is defined as the ratio of TPR (equivalent to sensitivity) to the FPR

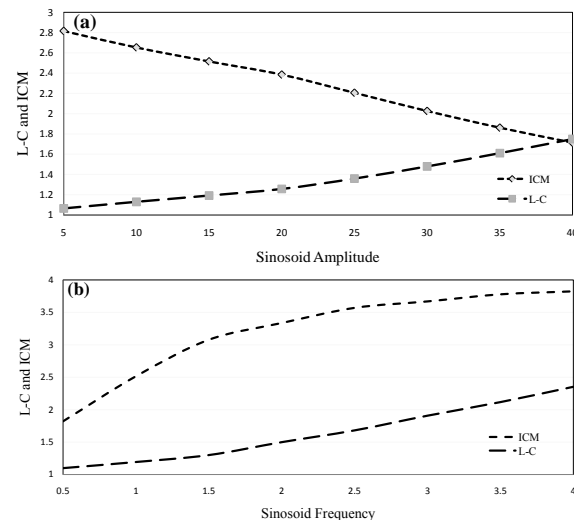


Fig. 5 Plot of inflection count metric (ICM) and L-C (arc-chord ratio) for (a) varying amplitude values and (b) varying frequency values.

(equal to $(1 - \text{specificity})$). The larger the values of PPV, NPV and PLR, the better the performance of the tortuosity index using the given classifier. Using the NB classifier, the maximum values of PPV, NPV and PLR are for ' τ ' metric followed by K_{tc}/C and K_{tc}/L and the minimum values of PPV, NPV, and PLR are for K_{tc} metric. Using the NN classifier, the maximum values of PPV and PLR are for K_{tc}/C and K_{tc}/L followed by ' τ ' metric and the maximum values of NPV are for ' τ ' metric followed by K_{tc}/C and K_{tc}/L and the minimum values of PPV, NPV and PLR are for K_{tsc} and K_{tsc}/L . The predictive values of a test result are dependent on the prevalence of the disease in the patients being tested unlike the area under the curve (AUC), of the receiver operating characteristic plot. The AUC does not take into account the prevalence (prior probability) of the disease; it provides a composite measure of test accuracy and is not dependent on an arbitrary interpretive threshold, therefore it is not used as a discriminability test in this work.

RESULTS

Simulation results

The various tortuosity measures evaluated on the simulated vessel sets are shown in Figs. 5–7.

In Fig. 5a, as the sinusoid amplitude changes, a valid tortuosity measure is expected to increase with increasing amplitude. The value of frequency is fixed at $f = 1$. The figure indicates that L-C measure is sensitive to such changes. Whereas ICM follows the

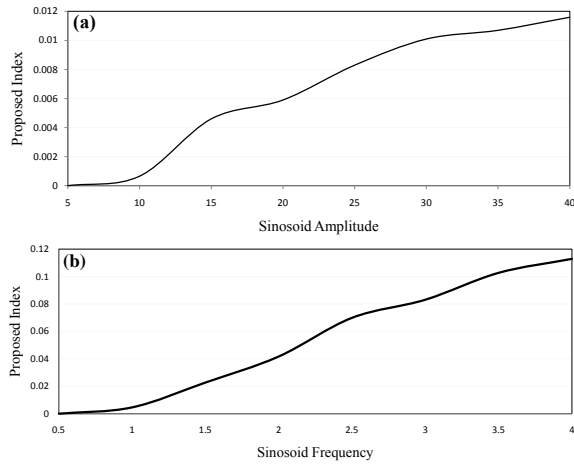


Fig. 6 Plot of integrated proposed index, τ , for (a) varying amplitude values and (b) varying frequency values.

reverse trend for amplitude modulation (changes in amplitude), that is to say it decreases for increase in amplitude at fixed frequency.

Fig. 5b demonstrates the course for the putative indices, ICM and L-C for frequency changes. The value of amplitude considered is $A = 15$. The ICM index follows frequency modulation, except when $A = 40$ is considered and for $f = 4$, indicating that it does not prove reliable at higher amplitudes, on the other hand, L-C measure follows the expected trend for frequency modulation, that is to say it increases for increase in frequency at fixed amplitude. Hence it is concluded that both fulfil frequency modulation criterion.

Fig. 6 shows the trend of the proposed index, τ . It is observed that the index increases as the amplitude is increased at fixed frequency. The value of frequency, $f = 1$, (Fig. 6a). It depicts the same trend for frequency changes, i.e., it increases as the frequency of the simulated vessels are increased at fixed amplitude, $A = 15$, indicating that it fulfils the criterion of frequency modulation (Fig. 6b). Hence the index fulfils the criteria of amplitude modulation as well as frequency modulation.

Fig. 7a shows that the index, total curvature, K_{tc} and total squared curvature; K_{tsc} follows the expected trend for amplitude modulation, though the K_{tsc} measure shows somewhat small changes. Hence both fulfil the criteria of amplitude modulation.

Fig. 7b depicts the trend for the indices, K_{tc} and K_{tsc} for frequency changes. It increases in the same manner as Fig. 7a, but with a better slope. Thus fulfils the frequency modulation property.

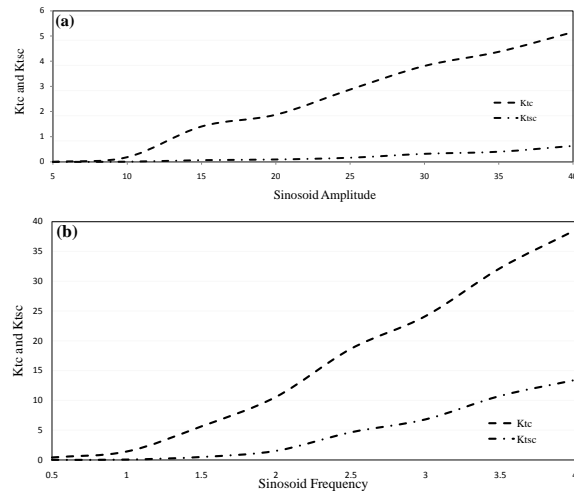


Fig. 7 Plot of total curvature, K_{tc} , and total squared curvature, K_{tsc} , based on curvature estimates of improved chain code, for (a) varying amplitude values and (b) varying frequency values.

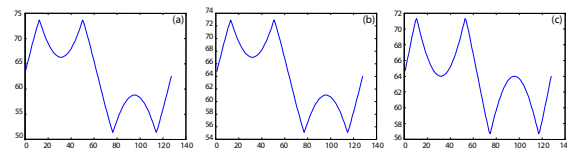


Fig. 8 Sine waves flipped at (a) 0.7, (b) 0.6, and (c) 0.5, respectively.

A special case of flipped sinusoids (Fig. 8) is also tested on the available and the proposed indices and found that the proposed indices are sensitive to shape²². The metrics L-C, ICM, K_{tsc} are scale invariant, since the values remains nearly the same, whereas τ and K_{tc} indices are scale-variant by a factor $1/\gamma^5$. Another property which an ideal index should satisfy is termed as additive property. The tortuosity of a vessel comprising several parts should be given by adding together the tortuosity values of the constituent segments. We observe (from previous experiments) that our proposed metrics are additive²².

Table 2 compares the properties of our proposed metrics with two other previously proposed indices. The L-C ratio commonly used as an index of tortuosity only indicates vessel elongation and has no value in measuring morphology or haemodynamic consequences. The ICM measure also cannot differentiate between different shapes as it remains constant. Our proposed indices behave consistently with intuitive notions of tortuosity.

Table 2 A comparison of the tortuosity indices with respect to the required properties (-do- indicates that an index shows the required property; -x- indicates that it does not).

	L-C	ICM	K_{tc}	K_{tsc}	τ
Additive	-x-	-x-	-do-	-do-	-do-
Modulation	-do-	-do-	-do-	-do-	-do-
Shape	-x-	-x-	-do-	-do-	-do-
Scaling	-do-	-do-	-x-	-do-	-x-

Table 3 Classification accuracy of our K_{tc} and K_{tsc} tortuosity metrics for different values of k using NB and NN classifiers.

k	2	3	4	5	6	7	8	10
K_{tc} , NB	56.4	59.3	55.0	55.0	50.0	43.6	35.7	27.1
K_{tc} , NN	66.4	67.1	69.3	68.6	74.3	68.6	67.9	70.7
K_{tsc} , NB	53.6	50.7	38.6	40.7	45.0	42.1	40.1	38.6
K_{tsc} , NN	61.4	63.6	66.4	66.3	62.9	64.3	62.1	61.4

Classification results

Table 3 depicts the classification accuracy of our K_{tc} and K_{tsc} metrics for different values of k . Table 4 and Table 5 give the performance comparison of the two classifiers. We show results for our proposed metrics and two existing measures, the L-C measure and ICM. Results indicate that the NB classifier performs substantially better in specificity, accuracy, PPV, NPV and PLR than the NN classifier for the normalized total squared curvature measure. Whereas, the NN classifier performs better in accuracy and specificity than NB for all the other proposed metrics with the best sensitivity, specificity, accuracy, PPV, NPV, and PLR values of 84.4%, 95.7%, 90.1%, 90.5%, 92.6% and 19.4, respectively, for the chord length normalized total curvature metric, K_{tc}/C , and the best sensitivity and accuracy values of 97.8% and 93.6% for the integrated proposed index, τ . However, values of PPV, NPV, and PLR reveal that the best possible prediction is achieved using NB classifier for the τ metric.

DISCUSSION

In this study, numerical methods are developed to quantify deformity in the retinal blood vessels of premature infants. It is to be noted that in two-dimensional fundus images, vessels with high curvature are an important attribute of tortuosity. The location and the number of the highly kinked vessels provide good representation of the tortuosity in the image. The measure K_{tsc} differs from K_{tc} as it places greater emphasis on parts of curve that have high curvature and de-emphasizes the parts of the

Table 4 Performance comparison of the tortuosity indices at segmental level using a naïve Bayes classifier.

Metric	Naïve Bayes classifier					
	Sensi- tivity (%)	Speci- ficity (%)	Accu- racy (%)	PPV (%)	NPV (%)	PLR
L-C	57.1	84.8	72.9	63.2	81.3	3.75
ICM	51.9	79.3	62.1	42.4	84.9	2.51
τ	86.7	96.7	91.4	92.9	93.7	26.5
K_{tc}	37.5	44.6	35.7	15.0	73.2	0.676
K_{tsc}	45.8	48.9	40.1	19.0	77.6	0.897
K_{tc}/L	82.6	94.6	89.3	88.4	91.6	15.2
K_{tc}/C	84.1	95.7	89.3	90.2	92.6	19.3
K_{tsc}/L	31.0	88.0	67.1	54.2	73.6	2.58
K_{tsc}/C	47.5	80.4	66.4	59.4	77.9	2.43
Average	58.3	79.2	68.3	58.3	82.9	8.20
S.D.	22.5	19.5	20.4	29.2	8.1	9.58

Table 5 Performance comparison of the tortuosity indices at segmental level using KNN classifier.

Metric	KNN classifier					
	Sensi- tivity (%)	Speci- ficity (%)	Accu- racy (%)	PPV (%)	NPV (%)	PLR
L-C	46.5	89.1	72.9	66.7	78.1	4.28
ICM	77.3	90.2	83.6	79.1	89.2	7.89
τ	97.8	93.5	93.6	88.2	98.9	15.0
K_{tc}	30.4	88.0	67.9	56.0	71.7	2.54
K_{tsc}	57.1	68.5	62.1	45.3	77.8	1.81
K_{tc}/L	81.8	95.7	88.6	90.0	91.7	18.8
K_{tc}/C	84.4	95.7	90.1	90.5	92.6	19.4
K_{tsc}/L	37.0	79.3	64.3	47.2	71.6	1.79
K_{tsc}/C	50.0	76.1	65.0	48.8	76.9	2.09
Average	62.5	86.2	76.4	68.0	83.2	8.17
S.D.	23.6	9.5	12.5	19.3	10.0	7.50

curve with low curvature, similar to the measures τ_3 and τ_2 proposed by Hart et al⁵ except that the latter directly calculated the curvature of the curve. Since small vessels have greater curvature, the measure K_{tsc} emphasizes the tortuosity of such vessels more than K_{tc} . Thus the proposed metric proved to be most resilient to very noisy images and small or especially tortuous blood vessels, which makes it well-suited for implementation as a tortuosity assessment tool in automatic software for retinal vessel analysis. Based on experiments with simulated curves, it is inferred that the metric is sensitive to changes in shape of the vessels (Fig. 8) and fulfils additive property unlike L-C and ICM metric and satisfies all the abstract

properties of a valid tortuosity index as compared to the previously proposed indices (Table 2). The integrated proposed tortuosity index τ is tested for different values of k using NB and NN classifiers (Table 1). The value of $k = 8$ results in the highest classification accuracy with both the classifiers. Thus the highest values of different performance measures for the τ metric (sensitivity, specificity, PPV, NPV, PLR, and accuracy) are attributed to this fact. We found that the sensitivity and specificity of the integrated proposed index was superior to that of the two existent tortuosity metrics, L-C and ICM using both classifiers. This implies that there are few false negatives or few instances, where plus disease exists and the proposed index fails to detect it and very few false positives detected that could lead to unnecessary laser treatment. High sensitivity and high specificity is possibly the most desirable feature of a diagnostic test for plus disease in ROP to reduce the risk of delayed treatment and retinal detachment. It should also be noted that the existent metric shows reduced sensitivity and high specificity, indicating that it results in more false positives. Even the less tortuous segments are wrongly detected as tortuous segments, which would consequently result in unnecessary laser treatment. Other performance measures also show improved performance as compared to the L-C and ICM metrics on our experimental dataset.

Using the KNN classifier, the maximum values of PPV and PLR are 90.5% and 19.4 for K_{tc}/C , and those of accuracy and NPV are 93.6% and 98.9% for the τ metric and the minimum values of accuracy, PPV, NPV, and PLR are 62.1% and 45.3% for K_{tsc} and 71.6% and 1.79 for K_{tsc}/L , respectively. Using the NB classifier, the maximum values of accuracy, PPV, NPV, and PLR are 91.4%, 92.9%, 93.7% and 26.5, respectively, for τ metric, and the minimum values of accuracy, PPV, NPV, and PLR are 35.7%, 15.0%, 73.2% and 0.676 for K_{tc} metric. The detailed results of performance measurements using NB and NN classifiers, and average values and standard deviation using all of the nine metrics are presented in Table 4 and Table 5.

Nonetheless, results obtained by our K_{tc} and K_{tsc} metrics over varying regions of support, i.e., for different values of k , using the two different classifiers corresponds to different values of accuracy. The K_{tc} metric attains the highest accuracy values for $k = 3$ with NB classifier and $k = 6$ with NN classifier (Table 3). On the other hand, the K_{tsc} metric achieves the best classification rate at $k = 2$ with NB and $k = 4$ with NN classifier (Table 3). We used $k = 8$ for our analysis with all the metrics, since clinicians usually

do not consider vessels of pixels less than 10 for tortuosity evaluation, consequently the K_{tc} and K_{tsc} metrics result in low values of accuracy, sensitivity, specificity, PPV, NPV, and PLR (Table 4 and Table 5). Nevertheless, the corresponding normalized metrics achieves appreciable improvement in the values of different performance measures. This shows that curvature-based (improved k -curvature) metrics rely heavily on the accurate determination of the local region of support. We considered arterioles and venules alike in this study following Johnston et al³⁰, which resulted in high diagnostic accuracy when considering tortuosity sufficient for pre-plus or plus disease with the assessment of arterioles alone and arterioles and venules together.

In comparison to other published methods, the proposed metrics can estimate appropriate tortuosity for vessels with constant or changing curvature juxtaposed the earlier proposed metrics^{3,4}. The proposed approach provides good discrimination between vessels of different tortuosity and hence could be used as an analytical tool in automated software for grading of tortuosity. The number of inflection points could vary for images of different sizes and pathologies for our τ metric. Notwithstanding the fact, the proposed method depends on image resolution, it poses no problem when comparing vessels of similar calibres. The proposed metric is independent of the method of segmentation of the vessel tree. Hence problems arising due to vessel bifurcation, crossing and branching are correctly identified, so that vessel course may be fully reconstructed. The method obviates the need of smoothing required due to the presence of noise and discrete nature of the pixel representation. It reduces the error in tortuosity calculation arising due to low quality image of the retina, since the algorithm used to automatically extract the blood vessel segments is quite accurate with a specificity of 98.8% and a sensitivity of 89.4%⁹.

The proposed integrated index τ incorporates number of inflection points that in turn depends on image resolution, this limits the generalizability of the proposed metric. Another limitation of this metric is scale variance; therefore modifications would be required when a global measure for the entire retinal image needs to be computed. Our investigation on the metric quantification of tortuosity of fundus images is based on experts' graded ground truth data. Hence the issue of biased ascertainment poses limitation to this study. The evaluation remains within the boundaries of our experimental setup. All experiments are performed with our own implementations of the various measures. Comparisons are not candid as different

measures have different parameters.

We attempt to solve queries related to whether the segmentation method affects the tortuosity of the extracted vessels, whether the length of the extracted segments affects the utility of the tortuosity metrics, and how much of a role the extraction procedures play in the diagnosis. We conclude that the results would be helpful for work related to exploring the morphological properties of vessel population for healthy and diseased subjects.

CONCLUSIONS

In this paper, we have verified our integrated proposed index τ and a suite of curvature based (on improved chain code rules) tortuosity metrics quantitatively by comparing results of tortuosity estimation with ophthalmologists' graded ground truth retinal segmental vessels. Two of the methods proposed in literature to estimate retinal vessel tortuosity have been implemented and comparatively evaluated in the present work (in terms of abstract properties of a valid tortuosity metric). The proposed approach is computationally simpler compared to other existing measures and proved most accurate to describe the ophthalmologist's perception of retinal vessel tortuosity, in case of ROP. Our approach aims to measure the correctness of the algorithms at the segmental level. While our results are encouraging, for other diseases modifications could be made as appropriate. Investigations are underway to assess the validity of the proposed metrics in other retinopathies with comparable vascular morphology changes, such as diabetic retinopathy and cardiovascular diseases.

As part of our future work, that also includes further validation on a larger number of vessel samples, validation from multiple clinicians, and a sound understanding of the diagnostic values of automatic tortuosity measures, we intend to provide a global tortuosity index for the entire retinal image.

Acknowledgements: The authors are grateful to Digital Imaging Research Centre, Kingston University, London, Department of Ophthalmology, Imperial College, London and Thammasat Hospital, Thailand for providing the retinal images for the project. The authors also like to extend their gratitude to Thammasat eye Centre for providing the necessary support in grading the images segment wise.

REFERENCES

1. Wong TY, Klein R, Couper DJ, Cooper LS, Shahar W, Hubbard LD, Wofford MR, Sharret AR (2001) Retinal microvasculature abnormalities and incident stroke: The atherosclerosis risk in communities study. *Lancet* **358**, 1134–40.
2. Capowski JJ, Kylstra JA, Freedman SF (1995) A numeric index based on spatial frequency for the tortuosity of retinal vessels and its application to plus disease in retinopathy of prematurity. *Retina* **15**, 490–500.
3. Bullit E, Gerig G, Pizer S, Lin W, Aylward S (2003) Measuring tortuosity of the intracerebral vasculature from MRA images. *IEEE Trans Med Imag* **22**, 1163–71.
4. Lotmar W, Freiburghaus A, Bracher D (1979) Measurement of vessel tortuosity on fundus photographs. *Graefe's Arch Clin Exp Ophthalmol* **211**, 49–57.
5. Hart WE, Goldbaum M, Cote B, Kube P, Nelson MR (1999) Automated measurement of retinal vascular tortuosity. *Int J Med Informat* **53**, 239–52.
6. Aslam T, Fleck B, Patton N, Trucco M, Azegrouz H (2009) Digital image analysis of plus disease in retinopathy of prematurity. *Acta Ophthalmol* **87**, 368–77.
7. Bracher D (1986) Changes in peripapillary tortuosity of the central retinal arteries in new borns. *Graefe's Arch Clin Exp Ophthalmol* **218**, 211–7.
8. Heneghan C, Flynn J, Keefe MO, Cahill M (2000) Characterization of changes in blood vessel width and tortuosity in retinopathy of prematurity using image analysis. *Med Image Anal* **6**, 407–29.
9. Sukkaew L, Uyyanonvara B, Makhonov SS, Barman S, Panguthipong P (2008) Automatic tortuosity-based retinopathy of prematurity screening system. *IEICE Trans Info Syst* **91**, 2868–74.
10. Kylstra JA, Wierzbicki T, Wolbarst ML, Landers MB III, Steffansson E (1986) The relationship between retinal vessel tortuosity, diameter and transmural pressure. *Graefe's Arch Clin Exp Ophthalmol* **224**, 477–80.
11. Kaupp A, Toonen H, Wolf S, Schulte K, Effert R, Meyer-Ebrecht D, Reim M (1991) Automatic evaluation of retinal vessel width and tortuosity in digital fluorescein angiograms. *Investig Ophthalmol Vis Sci* **32**, 952.
12. Martin Rodriguez Z, Kenny P, Gaynor L (2011) Improved characterisation of aortic tortuosity. *Med Eng Phys* **33**, 712–9.
13. Dougherty G, Varro J (2000) A quantitative index for the measurement of the tortuosity of blood vessels. *Med Eng Phys* **22**, 567–74.
14. Gao XW, Bharath A, Stanton A, Hughes A, Chapman N, Thom S (2000) Quantification and characterisation of arteries in retinal images. *Comput Meth Programs Biomed* **63**, 133–46.
15. Pedersen L, Grunkin M, Ersbüll B, Madsen K, Larsen M, Christofersen N, Skands U (2000) Quantitative measurement of changes in retinal vessel diameter in ocular fundus images. *Pattern Recogn Lett* **21**, 1215–23.
16. Grisan E, Foracchia M, Ruggeri A (2008) A novel method for the automatic grading of retinal vessel tortuosity. *IEEE Trans Med Imag* **27**, 310–9.
17. Wallace DK (2007) Computer-assisted quantification

- of vascular tortuosity in retinopathy of prematurity (an American Ophthalmological Society thesis). *Trans Am Ophthalmol Soc* **105**, 594–615.
18. Wilson CM, et al (2008) Computerized analysis of retinal vessel width tortuosity in premature infants. *Investig Ophthalmol Vis Sci* **49**, 3577–85.
 19. Johnson MJ, Dougherty G (2007) Robust measures of three-dimensional vascular tortuosity based on the minimum curvature of approximating polynomial spline fits to the vessel mid-line. *Med Eng Phys* **29**, 677–90.
 20. Turior R, Onkaew D, Uyyanonvara B (2013) PCA-based retinal vessel tortuosity quantification. *IEICE Trans Info Syst* **E96.D**, 329–39.
 21. Onkaew D, Turior R, Uyyanonvara B, Akinori N, Sinthanayothin C (2011) Automatic retinal vessel tortuosity measurement using curvature of improved chain code. In: *Proceedings of the International Conference on Electrical, Control and Computer Engineering (In-ECCE 2011)*, pp 183–6.
 22. Turior R, Onkaew D, Uyyanonvara B (2011) Robust metrics for retinal vessel tortuosity measurement using curvature based on improved chain code. In: *Proceedings of the International Conference on Biomedical Engineering (ICBME 2011)*, pp 217–21.
 23. Pal S, Bhowmick P (2009) Estimation of discrete curvature based on chain-code pairing and digital straightness. In: *Proceedings of the 2009 IEEE International Conference on Image Processing*, pp 1097–100.
 24. Smedby O, Hogman N, Nilsson S, Erikson U, Olsson AG, Walldius G (1993) Two-dimensional tortuosity of the superficial femoral artery in early atherosclerosis. *J Vasc Res* **30**, 181–91.
 25. Teh CH, Chin RT (1989) On the detection of dominant points on digital curves. *IEEE Trans Pattern Anal Mach Intell* **11**, 859–72.
 26. An International Committee for the Classification of Retinopathy of Prematurity (2005) The International Classification of Retinopathy of Prematurity revisited. *Arch Ophthalmol* **123**, 991–9.
 27. Trucco E, et al (2010) Modelling the tortuosity of retinal vessels: Does calibre play a role? *IEEE Trans Biomed Eng* **57**, 2239–47.
 28. Friedman N, Geiger D, Goldszmidt M (1997) Bayesian network classifiers. *Mach Learn* **29**, 131–63.
 29. Richard DD, Peter EH, David GS (2000) *Pattern Classification* 2nd edn, A Wiley-Interscience Publication, pp 20–83.
 30. Johnston SC, et al (2009) Tortuosity of arterioles and venules in quantifying plus disease. *J AAPOS* **13**, 181–5.